

Next-to-leading order QCD corrections to the Z boson pair production at the LHC in Randall Sundrum model.

Neelima Agarwal^{a 1}, V. Ravindran^{b 2}, Vivek Kumar Tiwari^{a 3}, Anurag Tripathi^{b 4}

a) *Department of Physics, University of Allahabad, Allahabad 211002, India.*
 b) *Regional Centre for Accelerator-based Particle Physics,
 Harish-Chandra Research Institute, Chhatnag Road, Jhunsi, Allahabad 211019, India.*

Abstract

The first results on next-to-leading order QCD corrections to production of two Z bosons in hadronic collisions in the extra dimension model of Randall and Sundrum are presented. Various kinematical distributions are obtained to order α_s in QCD by taking into account all the parton level subprocesses. We estimate the impact of the QCD corrections on various observables and find that they are significant. We also show the reduction in factorization scale uncertainty when $\mathcal{O}(\alpha_s)$ effects are included.

¹neel1dph@gmail.com

²ravindra@hri.res.in

³vivekkrt@gmail.com

⁴anurag@hri.res.in

1 Introduction

The last missing piece of the standard model (SM), the Higgs boson, remains elusive to this date, and it is hoped that the Large Hadron Collider (LHC) will shed light on the mechanism of spontaneous symmetry breaking and discover the Higgs bosons. Even if it is discovered there remain fundamental issues, such as the hierarchy problem and others, which make us believe in the existence of some new physics beyond the standard model. The LHC which will operate at an enormous centre of mass energy ($\sqrt{S} = 14$ TeV) promises to be a discovery machine and it is hoped that some signals of new physics beyond the SM will be observed. Extra dimension models [1–4] offer an attractive alternative to the supersymmetry to address the hierarchy problem. In this paper we will consider the extra dimension model of Randall and Sundrum (RS) [3, 4]. There are many important discovery channels at the LHC such as $\gamma\gamma$, ZZ , W^+W^- , jet production. In the SM the production of two Z bosons is suppressed as it begins at the order e^4 in the the electromagnetic coupling and also because of the large ZZ production threshold. The two Z bosons can couple to Kaluza Klein (KK) gravitons, thus ZZ pairs can be produced through virtual graviton exchange at the leading order. These observations make ZZ production one of the important discovery channels.

At hadron colliders Quantum Chromodynamics (QCD) plays an important role as the *incoming* states in any scattering event are the partons, which are described by parton distribution functions (pdf^s). The pdf^s depend on the factorization scale (μ_F) which is, to a large extent, arbitrary. This scale μ_F enters into any observable and makes it sensitive to the choice of its value and any leading order computation suffers from this sensitivity. However, as a computation beyond the leading order (LO) is carried out, the μ_F dependence partially cancels yielding results less sensitive to the factorization scale. It also improves upon LO results in that it includes missing higher orders terms of the perturbation series which can be large. It is, thus, the motivation of this paper to consider production of Z boson pairs at the LHC at next-to-leading

order (NLO) accuracy in the strong coupling constant in RS model.

Leading order studies for ZZ production in the SM can be found in [5]. Z pair with a large transverse momentum jet at LO was studied in [6]. LO study for ZZ production in the context of extra dimension model of RS was carried out in [7] and coupling of radion with gluon and top quark loop was considered in [8]. Because of its importance ZZ production has also been studied to NLO accuracy in the SM [9–11]. These results were subsequently updated in [12, 13]. NLO studies in SM via gluon fusion were carried out in [14, 15]. These studies provide the precise estimate of higher order effects through K factor as well as the sensitivity of the predictions to factorization scale. Importantly, the corrections turned out to be larger than the expectations based on soft gluon effects justifying a full-fledged NLO computation taking into all the processes. We presented NLO results for ZZ production at the LHC in large extra dimension model of Arkani-Hamed, Dimopoulos and Dvali [1, 2] in [16] where it was shown that the K factors are large. Although NLO results are available in SM and ADD model they do not exist in literature in the context of RS model which is the material of the present paper.

The results which are presented in this paper are obtained using our NLO Monte Carlo code (which is implemented on FORTRAN 77) that can easily accommodate any cuts on the final state particles and obtain various kinematical distributions. Our code is based on the method of two cutoff phase space slicing (for a review of the method see [17]) to deal with soft and collinear singularities in the real emission contributions. We will use the matrix elements presented in [16] and refer the reader to this paper for further details.

In what follows we will first briefly describe the RS model and then present the numerical results and finally conclude.

2 RS Model

In the RS model the single extra dimension ϕ is compactified on a S^1/Z^2 orbifold with a radius R_c which is somewhat larger than the Planck length. Two 3-branes, the Planck brane and the TeV brane, are located at the orbifold fixed points $\phi = 0, \pi$, with the SM fields localized on the TeV brane. The five-dimensional metric, which is *non-factorizable* or *warped* is of the form

$$ds^2 = e^{-2\mathcal{K}R_c|\phi|} \eta_{\mu\nu} dx^\mu dx^\nu + R_c^2 d\phi^2 \quad (1)$$

where $0 \leq \phi \leq \pi$. The the huge ratio $\frac{M_{Pl}}{M_{EW}} \sim 10^{15}$ can be generated by the exponent $\mathcal{K}R_c$ which needs to be only of $\mathcal{O}(10)$ thereby providing a way of avoiding the hierarchy problem. It was shown in [18, 19] that R_c can be stabilized against quantum fluctuations by introducing an extra scalar field in the bulk.

The tower of massive Kaluza-Klein (KK) excitations of the graviton, $h_{\mu\nu}^{(n)}$, interact with the SM particles by:

$$\mathcal{L}_{int} \sim -\frac{1}{\overline{M}_{Pl}} T^{\mu\nu}(x) h_{\mu\nu}^{(0)}(x) - \frac{e^{\pi\mathcal{K}R_c}}{\overline{M}_{Pl}} \sum_{n=1}^{\infty} T^{\mu\nu}(x) h_{\mu\nu}^{(n)}(x) . \quad (2)$$

$T^{\mu\nu}$ is the symmetric energy-momentum tensor for the SM particles on the 3-brane, and \overline{M}_{Pl} is the reduced Planck scale. The masses of the $h_{\mu\nu}^{(n)}$ are given by

$$M_n = x_n \mathcal{K} e^{-\pi\mathcal{K}R_c} , \quad (3)$$

where the x_n are the zeros of the Bessel function $J_1(x)$. The zero-mode couples weakly and decouples but the couplings of the massive RS gravitons are enhanced by the exponential $e^{\pi\mathcal{K}R_c}$ leading to interactions of electroweak strength. Consequently, except for the overall warp factor in the RS case, the Feynman rules in the RS model are the same as those for the ADD case [20, 21]

The basic parameters of the RS model are

$$\begin{aligned} m_0 &= \mathcal{K} e^{-\pi\mathcal{K}R_c} , \\ c_0 &= \mathcal{K} / \overline{M}_{Pl} , \end{aligned} \quad (4)$$

where m_0 is a scale of the dimension of mass and sets the scale for the masses of the KK excitations, and c_0 is an effective coupling. The interaction of massive KK gravitons with the SM fields can be written as

$$\mathcal{L}_{int} \sim -\frac{c_0}{m_0} \sum_n^{\infty} T^{\mu\nu}(x) h_{\mu\nu}^{(n)}(x) . \quad (5)$$

Since \mathcal{K} is related to the curvature of the fifth dimension we need to restrict it to small enough values to avoid effects of strong curvature. On the other hand \mathcal{K} should not be too small compared to $\overline{M_{Pl}}$ because that would reintroduce hierarchy. These considerations suggest $0.01 \leq c_0 \leq 0.1$. For our analysis we choose to work with the RS parameters c_0 and M_1 the first excited mode of the graviton rather than m_0 .

Let us define $\mathcal{D}(Q^2)$ as the sum of KK graviton propagators

$$\mathcal{D}(Q^2) = \sum_{n=1}^{\infty} \frac{1}{Q^2 - M_n^2 + iM_n\Gamma_n} \equiv \frac{\lambda}{m_0^2} , \quad (6)$$

where M_n are the masses of the individual resonances (see Eq. 3) and the Γ_n are the corresponding widths. The graviton widths are obtained by calculating their decays into final states involving SM particles. λ is defined as

$$\lambda(x_s) = \sum_{n=1}^{\infty} \frac{x_s^2 - x_n^2 - i\frac{\Gamma_n}{m_0}x_n}{x_s^2 - x_n^2 + \frac{\Gamma_n}{m_0}x_n} , \quad (7)$$

where $x_s = Q/m_0$. We have to sum over all the resonances to get the value of $\lambda(x_s)$. This is done numerically and for a given value of x_s , we retain all resonances which contribute with a significance greater than one per mil, and treat the remaining KK modes as virtual particles (in which case the sum can be done analytically).

As the gravitons couple to Z bosons, $PP \rightarrow ZZ$ can now also proceed through a process where gravitons appear at the propagator level. These new channels make it possible to observe deviations from SM predictions if extra dimensions exist. In the following we will consider spin-2 gravitons only at the propagator level and investigate this process at NLO level.

3 Numerical results

In this section we present invariant mass (Q) and rapidity (Y) distribution of the Z boson pairs. These kinematical variables are defined as

$$Q^2 = (p_{Z_1} + p_{Z_2})^2, \quad Y = \frac{1}{2} \ln \frac{P_1 \cdot q}{P_2 \cdot q}, \quad (8)$$

where P_1 and P_2 are the momenta of colliding hadrons, and $q = p_{Z_1} + p_{Z_2}$ denotes the sum of the Z -boson 4-momenta. In obtaining these distributions all order α_s contributions have been taken into account. At leading order in SM, the process proceeds through $q\bar{q}$ initiated process. As the gravitons couple to the Z -bosons, $q\bar{q}$ and gg initiated processes with virtual gravitons also contribute at the same order in QCD. We have considered all the $q\bar{q}, gg$ initiated one loop virtual and, $q\bar{q}, qg, gg$ initiated real emission corrections to these processes, both in the SM and the gravity mediated processes, and their interferences. At the virtual level we used method of Passarino and Veltman [22] to reduce tensor loop integrals to scalar integrals. In dealing with real emission contributions we have used two cutoff phase space slicing method. Here, using two small dimensionless slicing parameters δ_s and δ_c , the singular (soft and collinear) regions of phase space are separated from the finite hard noncollinear region. We will refer to the sum of contributions to crosssection from virtual, soft and collinear regions as *2-body* contribution, and from hard noncollinear region as *3-body* contribution. The soft singularities cancel between real and virtual contributions and the collinear singularities were removed by mass factorization in \overline{MS} scheme, this gives the finite *2-body* contribution. Finally the kinematical distributions were obtained by integrating the *2-body*, *3-body* and leading order pieces over the phase space using monte carlo methods. Individually *2-body* and *3-body* contributions depend on the slicing parameters δ_s and δ_c but the sum is invariant against variations of these parameters over a wide range. For further analysis we will use $\delta_s = 10^{-3}$ and $\delta_c = 10^{-5}$. For further details please see [16].

Below we present various distributions for the LHC with a center of mass energy

of 14 TeV as a default choice. However we will also present some results for a center of mass energy of 10 TeV for the LHC. For numerical evaluation, the following SM parameters [23] are used

$$M_Z = 91.1876\text{ GeV}, \quad \sin^2 \theta_W = 0.231 \quad (9)$$

where θ_W is the weak mixing angle. For the electromagnetic coupling constant α we use $\alpha^{-1} = 128.89$. CTEQ6 [24, 25] density sets are used for parton distribution functions. 2-loop running for the strong coupling constant has been used, and we have done calculation with 5 quark flavors and taken the masses of quarks to be zero. The value of Λ_{QCD} is chosen as prescribed by the CTEQ6 density sets. At leading order we use CTEQ6L1 density set (which uses the LO running α_s) with the corresponding $\Lambda_{QCD} = 165\text{ MeV}$. At NLO we use CTEQ6M density set (which uses 2-loop running α_s) with the $\Lambda_{QCD} = 226\text{ MeV}$; this value of Λ_{QCD} enters into the evaluation of the 2-loop strong coupling. The default choice for the renormalization and factorization scale is the identification to the invariant mass of the Z boson pair ie., $\mu_F = \mu_R = Q$. Furthermore the Z bosons will be constrained to satisfy $|y_Z| < 2.5$, where y_Z is the rapidity of a final state Z boson .

In Fig. 1 we have plotted the invariant mass distribution both for the SM and the signal for LHC at 14 TeV . The two curves with peaks correspond to the signal and the remaining two curves give SM predictions. Here we have chosen $c_0 = 0.01$ and $M_1 = 1500\text{ GeV}$. To highlight the importance of QCD corrections we have also displayed the LO results of SM and the signal, and we observe that the K factors (defined as $K = d\sigma^{NLO}/d\sigma^{LO}$) are large. For the signal the K factor is 1.82 at $Q = 1500\text{ GeV}$. Also note that the gravitons appear as ever widening peaks, these resonance peaks are clear signals of the RS model as opposed to the enhancement of the tail in ADD model. Next we present in Fig. 2 the effects of varying the parameter c_0 on the invariant mass distribution. All the curves shown correspond to NLO results, and we have also plotted the SM background for comparison.

In Fig. 3 we have plotted the rapidity distribution $d\sigma/dY$ at LO and NLO both

for SM and the signal for $c_0 = 0.01$. We have plotted this distribution in the interval $-2.0 < Y < 2.0$ and have carried out an integration over the invariant mass interval $1450 < Q < 1550$ to increase the signal over the SM background. As expected the distribution is symmetric about $Y = 0$. In Fig. 4 we have shown the variation of rapidity distribution with c_0 .

We have mentioned before that the NLO QCD corrections reduce the sensitivity of the cross sections to the factorization scale μ_F ; this we now show in the Fig. 5. We have plotted SM and the signal both at LO and NLO, and have varied the factorization scale μ_F in the range $Q/2 < \mu_F < 2Q$. The central curve in a given band (shown by the dotted curves) correspond to $\mu_F = Q$. In all these results the renormalization scale is fixed at $\mu_R = Q$. We notice that the factorization scale uncertainty at NLO is much reduced compared to the LO. For instance at $Q = 1500 \text{ GeV}$ varying μ_F between $Q/2$ to $2Q$ shows a variation of 20.6% at LO for the signal, however the NLO result at the same Q value shows a variation of 7.1%. Similarly we show the dependence on factorization scale at LO and NLO in the rapidity distribution in Fig. 6 and Fig. 7 for SM and signal respectively.

At the end we present in Fig. 8, $d\sigma/dQ$ for LHC with a centre of mass energy of 10 TeV at NLO both for SM and signal. For comparison we have also plotted the 14 TeV results in the same figure.

4 Conclusions

In this paper we have carried out a full NLO QCD calculation for the production of two Z bosons at the LHC at 14 TeV in the extra dimension model of Randall and Sundrum. Here we take all order α_s contributions, both in the SM and in the gravity mediated processes and their interferences, into account. We have presented invariant mass and rapidity distributions both at LO and NLO. We use CTEQ 6L1 and CTEQ 6M parton density sets for LO and NLO observables, respectively. Significant enhancements over the LO predictions are observed. The K factors are found to be

large, for instance in invariant mass distribution the signal has a K factor of 1.82 at $Q = 1500\,GeV$ (the position of first resonance). We have also presented the effects of variation of parameter c_0 both in Q and Y distributions. We have shown that a significant reduction in LO theoretical uncertainty, arising from the factorization scale, is achieved by our NLO computation. For instance at $1500\,GeV$ varying μ_F between $Q/2$ to $2Q$ shows a variation of 20.6% at LO for the signal, however the NLO result at the same Q value shows a variation of 7.1%. Thus our NLO results are more precise than the LO results and suitable for further studies for constraining the parameters of the RS model. Invariant mass distribution is also presented for LHC at a center of mass energy of $10TeV$ at the NLO level.

Acknowledgments: The work of NA is supported by CSIR Senior Research Fellowship, New Delhi. NA, AT and VR would like to thank the cluster computing facility at Harish-Chandra Research Institute. NA and VKT also acknowledge the computational support of the computing facility which has been developed by the Nuclear Particle Physics Group of the Physics Department, Allahabad University under the Center of Advanced Study (CAS) funding of U.G.C. India. The authors would like to thank Prakash Mathews and M.C. Kumar for useful discussions.

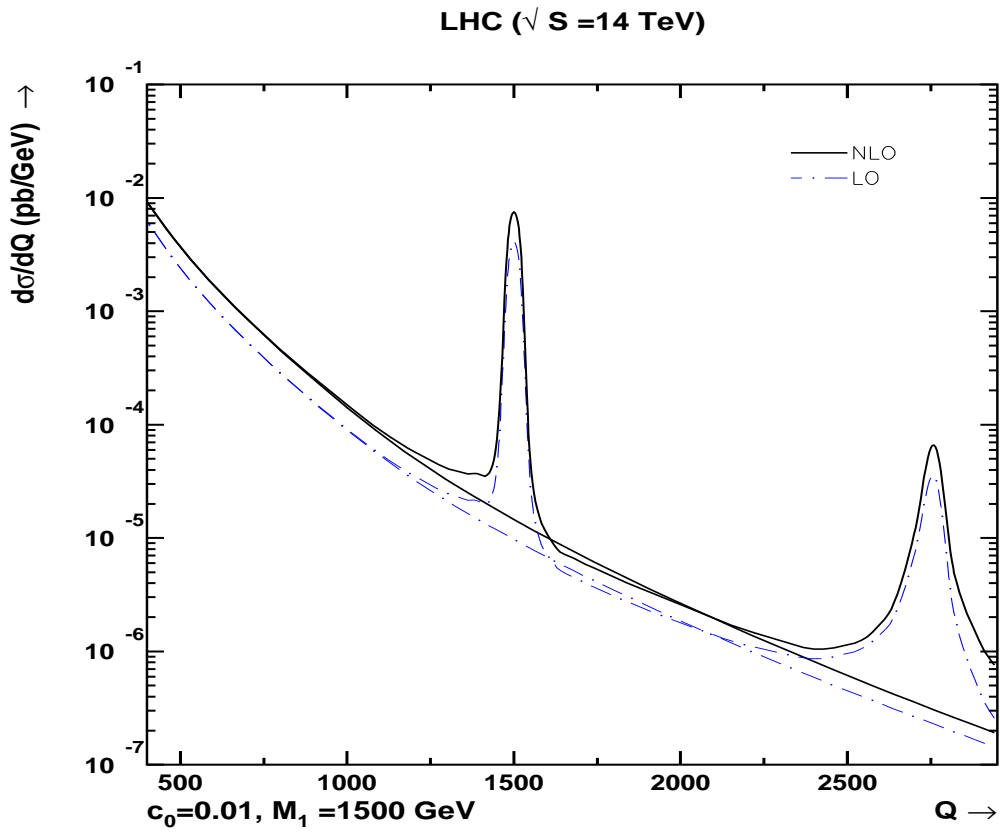


Figure 1: Invariant mass distribution for SM and signal both at LO and NLO. Dash-dot curves represent LO results and solid curves give NLO results. We have chosen $M_1 = 1500 \text{ GeV}$ and the parameter $c_0 = 0.01$.

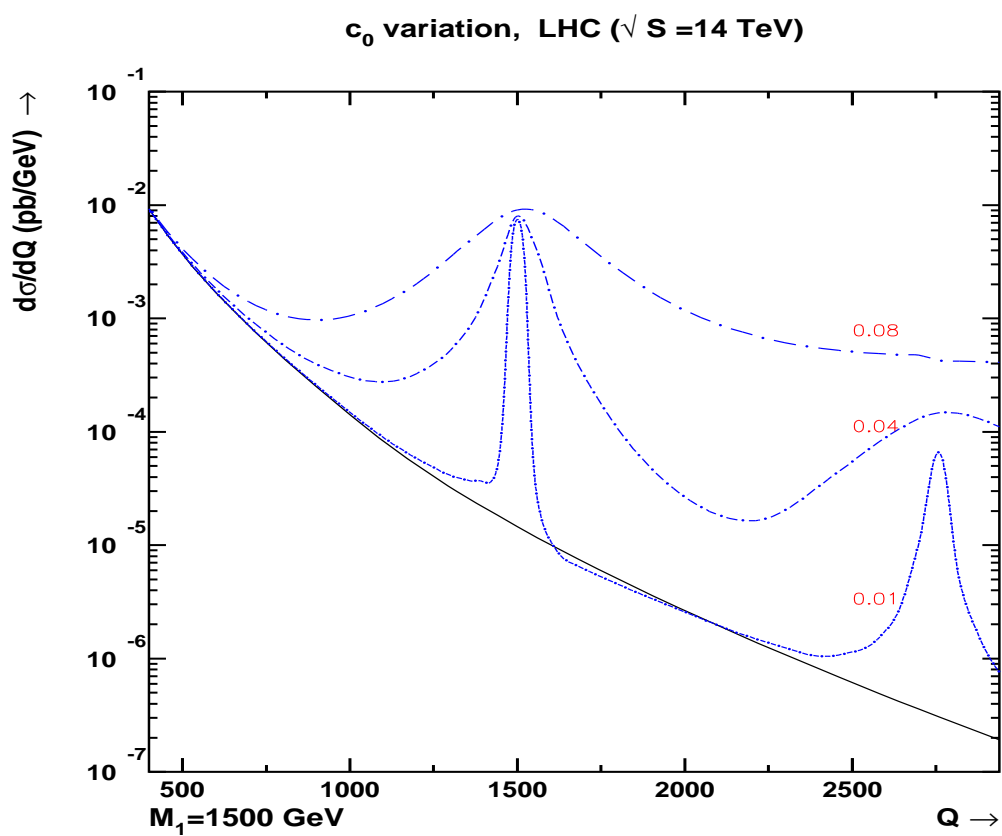


Figure 2: Effect of variation of c_0 on invariant mass distribution. All the curves correspond to NLO results with M_1 fixed at 1500 GeV. The solid curve corresponds to SM and the dash-dot curves to the signal. The signal is plotted for $c_0 = 0.01, 0.04, 0.08$ and the dash size increases with increasing c_0

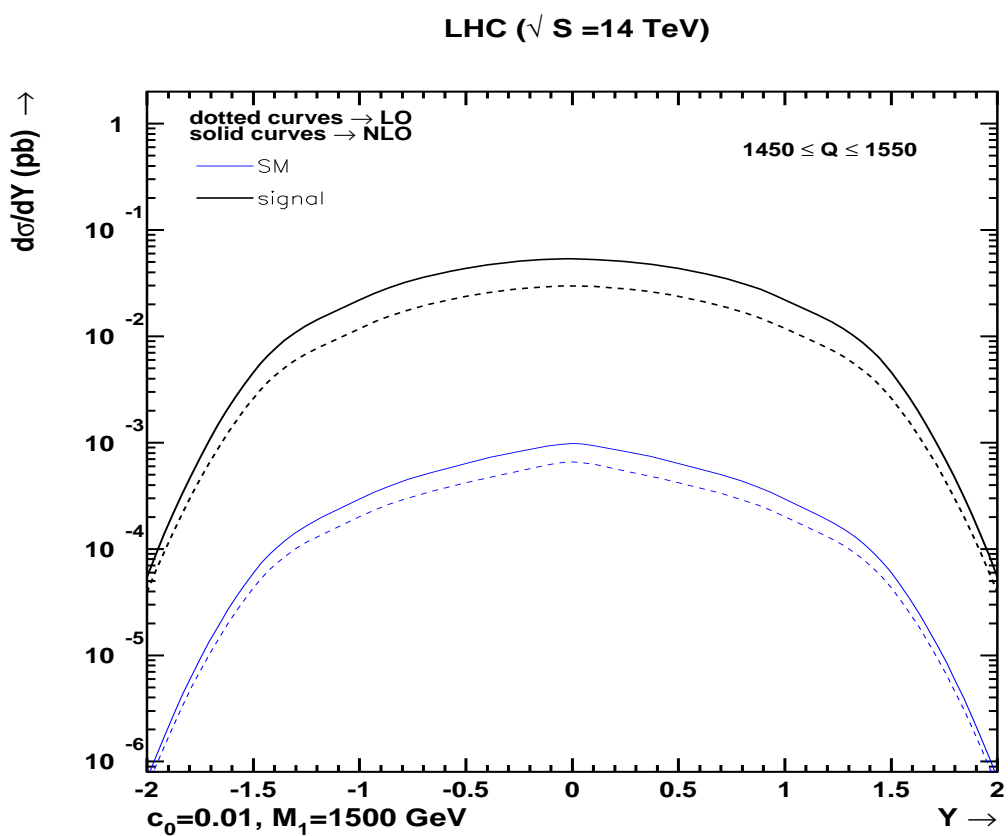


Figure 3: Rapidity distribution for SM and signal both at LO and NLO. Dash curves represent LO results and solid curves give NLO results. We have chosen $M_1 = 1500 \text{ GeV}$ and the parameter $c_0 = 0.01$. To enhance the signal we have integrated over Q in the range $1450 \leq Q \leq 1550$.

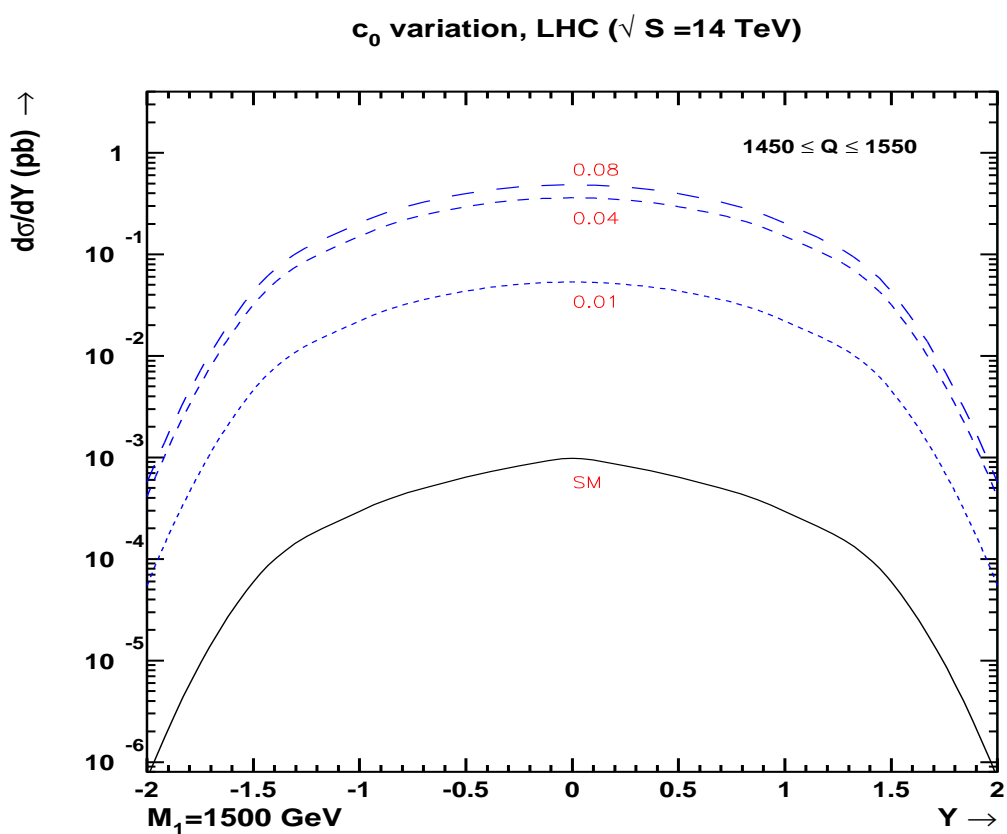


Figure 4: Rapidity distribution for SM and signal at NLO. Dash curves represent signal and solid curves gives SM contribution. We have chosen $M_1 = 1500$ GeV and plotted the signal for $c_0 = 0.01, 0.04, 0.08$. To enhance the signal we have integrated over Q in the range $1450 \leq Q \leq 1550$.

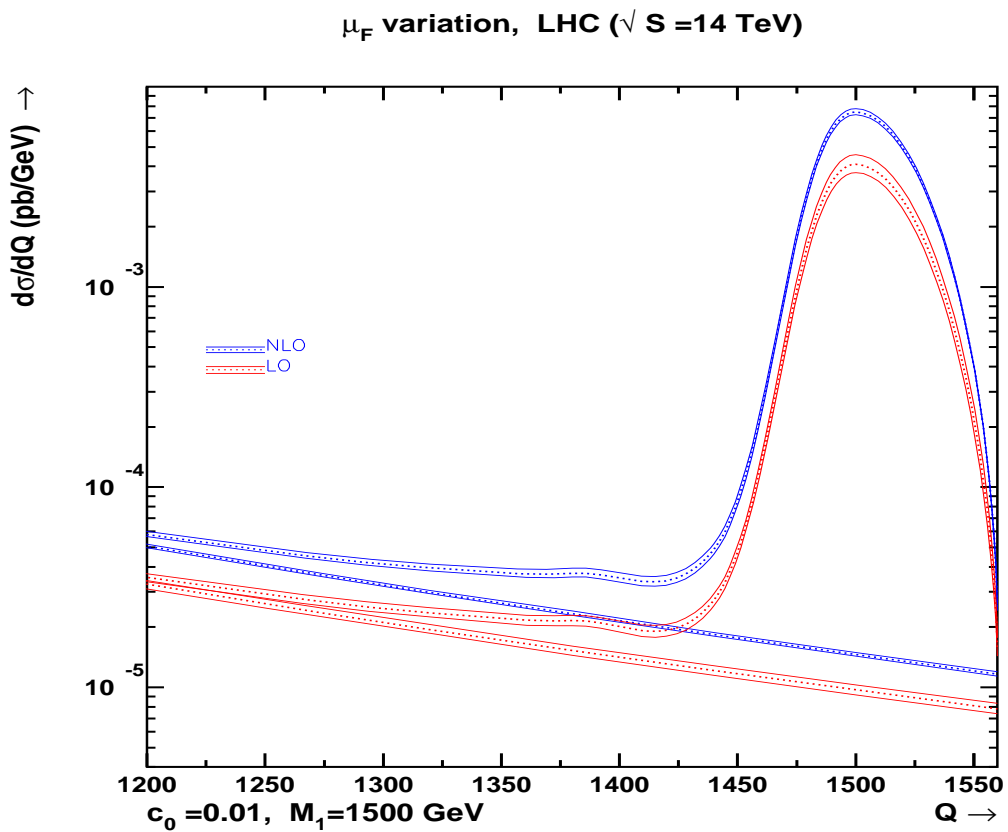


Figure 5: Factorization scale variation in the invariant mass distribution. The curves correspond to $c_0 = 0.01$ and $M_1 = 1500$ GeV at the LHC at $\sqrt{S} = 14$ TeV. The μ_F is varied between $Q/2$ and $2Q$. The dash curves correspond to $\mu_F = Q$

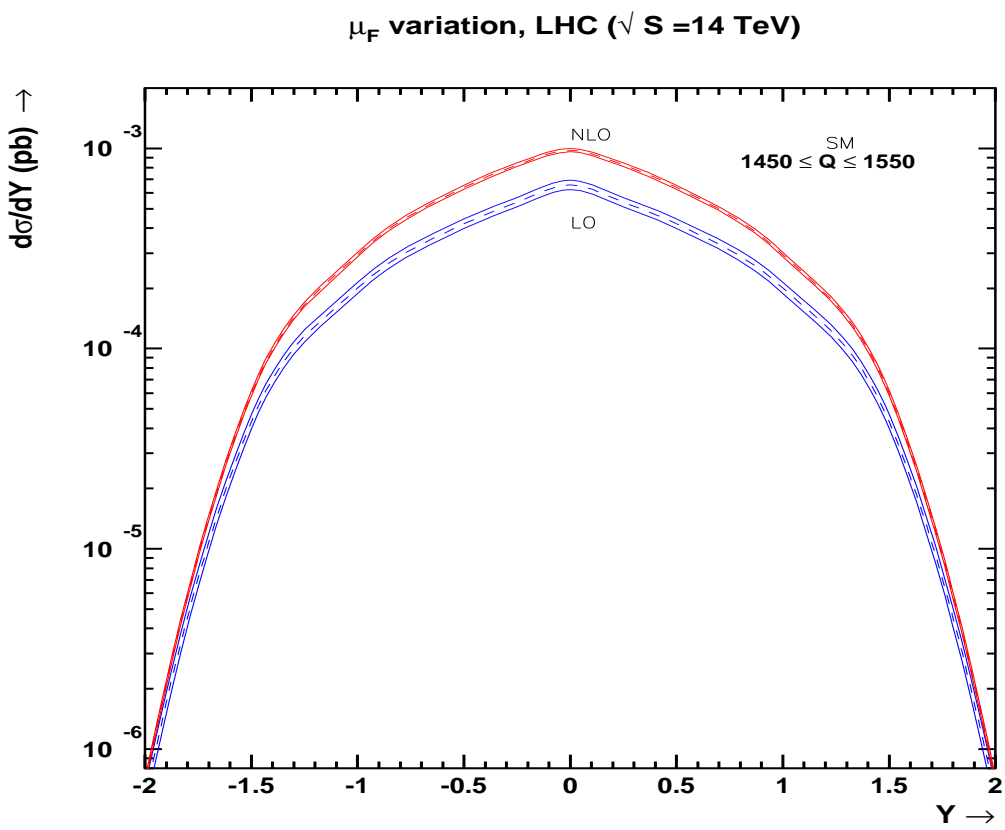


Figure 6: Factorization scale variation in the rapidity distribution for the SM. The curves correspond to $c_0 = 0.01$ and $M_1 = 1500\text{GeV}$ at the LHC at $\sqrt{S} = 14\text{TeV}$. To enhance the signal we have integrated over Q in the range $1450 \leq Q \leq 1550$. The μ_F is varied between $Q/2$ and $2Q$. The dash curves correspond to $\mu_F = Q$

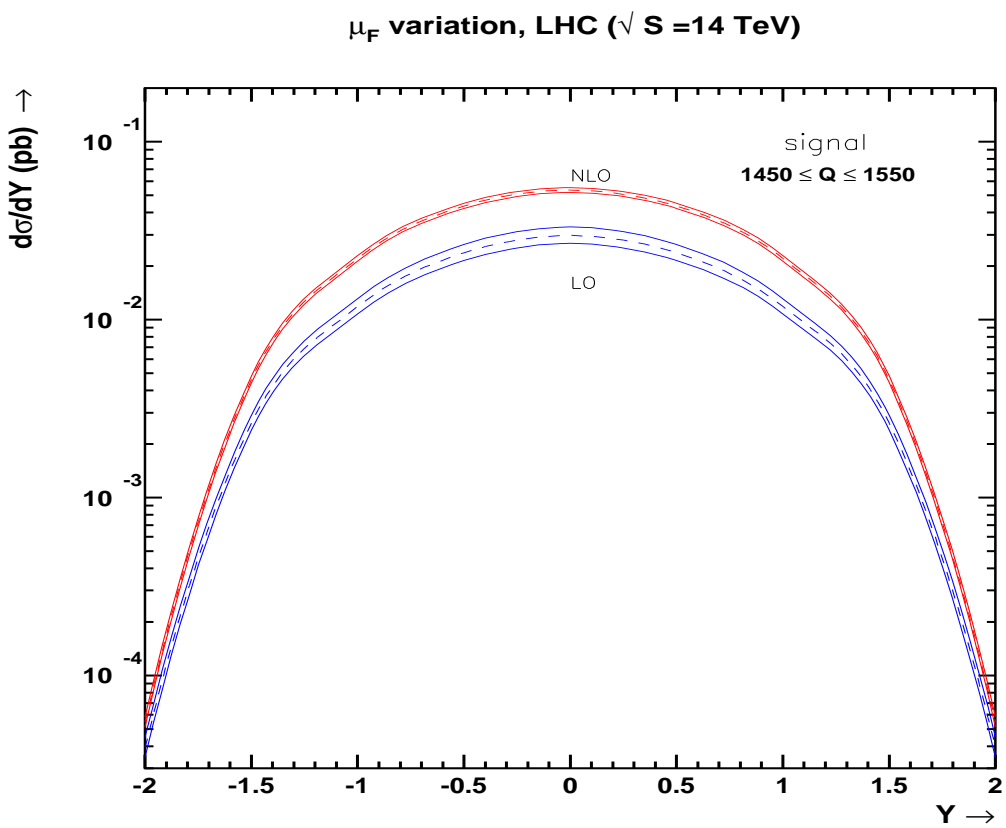


Figure 7: Factorization scale variation in the rapidity distribution for signal. The curves correspond to $c_0 = 0.01$ and $M_1 = 1500\text{GeV}$ at the LHC at $\sqrt{S} = 14$ TeV. To enhance the signal we have integrated over Q in the range $1450 \leq Q \leq 1550$. The μ_F is varied between $Q/2$ and $2Q$. The dash curves correspond to $\mu_F = Q$

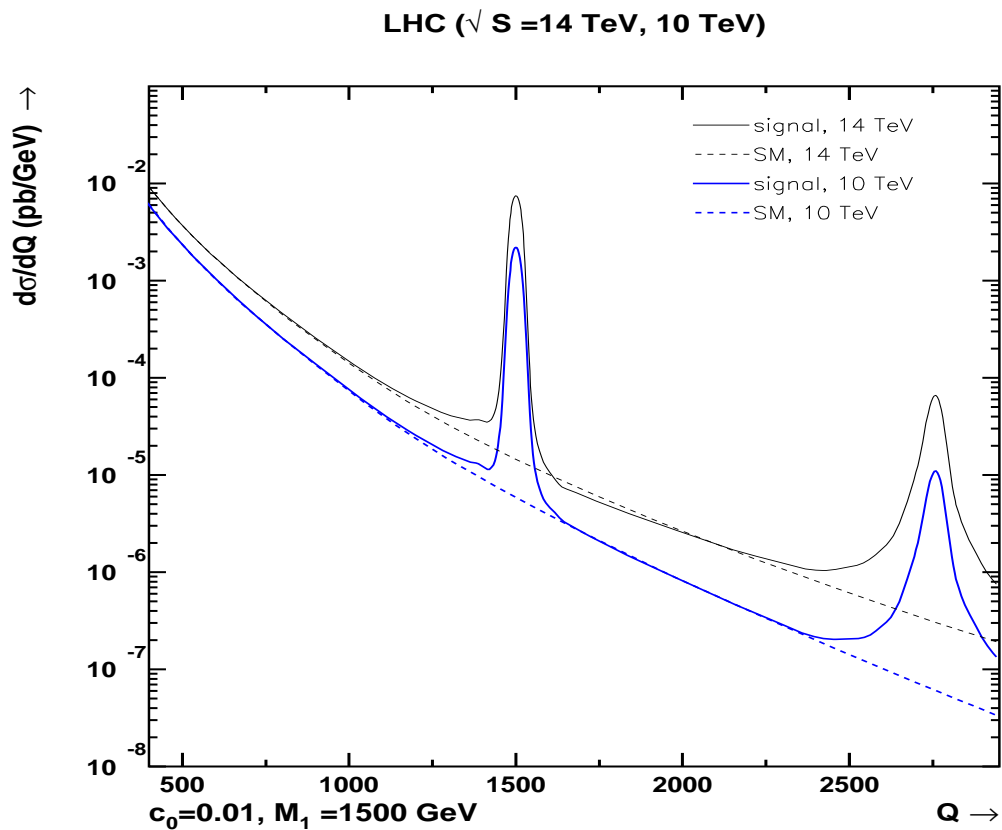


Figure 8: Invariant mass distribution for SM and signal at $\sqrt{S} = 10 \text{ TeV}$ and 14 TeV . All the curves correspond to NLO results. We have chosen $M_1 = 1500 \text{ GeV}$ and the parameter $c_0 = 0.01$.

References

- [1] I. Antoniadis, N. Arkani-Hamed, S. Dimopoulos and G. R. Dvali, Phys. Lett. B **436**, 257 (1998) [arXiv:hep-ph/9804398].
- [2] N. Arkani-Hamed, S. Dimopoulos and G. R. Dvali, Phys. Lett. B **429**, 263 (1998) [arXiv:hep-ph/9803315].
- [3] L. Randall and R. Sundrum, Phys. Rev. Lett. **83**, 3370 (1999) [arXiv:hep-ph/9905221].
- [4] L. Randall and R. Sundrum, Phys. Rev. Lett. **83**, 4690 (1999) [arXiv:hep-th/9906064].
- [5] R. W. Brown and K. O. Mikaelian, Phys. Rev. D **19** (1979) 922.
- [6] U. Baur, E. W. N. Glover and J. J. van der Bij, Nucl. Phys. B **318** (1989) 106.
- [7] S. C. Park, H. S. Song and J. H. Song, Phys. Rev. D **65**, 075008 (2002) [arXiv:hep-ph/0103308].
- [8] P. K. Das, Phys. Rev. D **72**, 055009 (2005) [arXiv:hep-ph/0508103].
- [9] J. Ohnemus and J. F. Owens, Phys. Rev. D **43**, 3626 (1991).
- [10] B. Mele, P. Nason and G. Ridolfi, Nucl. Phys. B **357**, 409 (1991).
- [11] B. Jager, C. Oleari and D. Zeppenfeld, Phys. Rev. D **73**, 113006 (2006) [arXiv:hep-ph/0604200].
- [12] L. J. Dixon, Z. Kunszt and A. Signer, Phys. Rev. D **60**, 114037 (1999) [arXiv:hep-ph/9907305].
- [13] J. M. Campbell and R. K. Ellis, Phys. Rev. D **60**, 113006 (1999) [arXiv:hep-ph/9905386].

- [14] E. W. N. Glover and J. J. van der Bij, Nucl. Phys. B **321**, 561 (1989).
- [15] T. Binoth, N. Kauer and P. Mertsch, arXiv:0807.0024 [hep-ph].
- [16] N. Agarwal, V. Ravindran, V. K. Tiwari and A. Tripathi, arXiv:0909.2651 [hep-ph].
- [17] B. W. Harris and J. F. Owens, Phys. Rev. D **65**, 094032 (2002) [arXiv:hep-ph/0102128].
- [18] W. D. Goldberger and M. B. Wise, Phys. Rev. Lett. **83**, 4922 (1999) [arXiv:hep-ph/9907447]; W. D. Goldberger and M. B. Wise, Phys. Lett. B **475**, 275 (2000) [arXiv:hep-ph/9911457].
- [19] C. Csaki, M. Graesser, L. Randall and J. Terning, Phys. Rev. D **62**, 045015 (2000) [arXiv:hep-ph/9911406]; C. Csaki, M. L. Graesser and G. D. Kribs, Phys. Rev. D **63**, 065002 (2001) [arXiv:hep-th/0008151].
- [20] G. F. Giudice, R. Rattazzi and J. D. Wells, Nucl. Phys. B **544** (1999) 3 [arXiv:hep-ph/9811291].
- [21] T. Han, J. D. Lykken and R. J. Zhang, Phys. Rev. D **59** (1999) 105006 [arXiv:hep-ph/9811350].
- [22] G. Passarino and M. J. G. Veltman, Nucl. Phys. B **160**, 151 (1979).
- [23] C. Amsler *et al.* [Particle Data Group], Phys. Lett. B **667**, 1 (2008).
- [24] J. Pumplin, D. R. Stump, J. Huston, H. L. Lai, P. M. Nadolsky and W. K. Tung, JHEP **0207** (2002) 012 [arXiv:hep-ph/0201195].
- [25] D. Stump, J. Huston, J. Pumplin, W. K. Tung, H. L. Lai, S. Kuhlmann and J. F. Owens, JHEP **0310** (2003) 046 [arXiv:hep-ph/0303013].